Helimagnet-based Non-volatile Multi-bit Memory Units

Rabiul Islam,[1,2] Peng Li,[3] Marijan Beg,[4] Manoj Sachdev,[1] and Guo-Xing Miao[1,2,a)]

[1)] *Department of Electrical and Computer Engineering, University of Waterloo,*
Waterloo,
Ontario N2L 3G1, Canada

[2)] *Institute for Quantum Computing, University of Waterloo,*
Waterloo,
Ontario N2L 3G1, Canada

[3)] *State Key Laboratory of Electronic Thin Film and Integrated Devices,*
University of Electronic Science and Technology of China, Chengdu 610054,
China

[4)] *Department of Earth Science and Engineering, Imperial College London,*
London SW7 2AZ, United Kingdom

(*Electronic mail: g2miao@uwaterloo.ca)

(Dated: 21 March 2023)

In this letter, we present a design of a helimagnet-based emerging memory device that is capable of storing multiple bits of information per device. The device consists of a helimagnet layer placed between two ferromagnetic layers, which allows us to lock in specific spin configurations. The bottom pinned layer has high anisotropy energy or stays exchange biased, which keeps its spin configuration fixed on a specific direction, while the top layer is free to rotate under the influence of in-plane fields. We begin by finding the relaxed spin structure, which is the result of the competition between the Dzyaloshinskii–Moriya interaction (DMI) and exchange energy and is referred to as the equilibrium state (“0”). The writing of a memory state is simulated by applying an in-plane field that rotates and transforms the spin configurations of the memory device. Our results indicate that stable configurations can be achieved at rotations of an integer multiple of 180 degrees (corresponding to states “-2”, “-1”, “1”, “2”, etc.), where the anisotropy stabilizes the free layer and thus the exchange coupled helimagnet. These states are separated by magnetic energy barriers and intermediate, unstable spin configurations tend to revert to their adjacent states. By simply changing the direction of the field, we can achieve multi-bit data storage per unit memory cell. The maximum number of bits is reached when the anisotropy energy barriers cannot withstand the strong DMI energy. Reading can be done by evaluating the different resistance states due to the twisted spin texture.

---

[a] http://miao.iqc.uwaterloo.ca/

Due to the advancement of information technology and computing, the use of electronic devices has been rapidly increasing. As all these devices have integrated memory systems, a substantial increase in their storage capacity has occurred to fill the growing need. Different memory devices, including existing and emerging memory, have been used to fulfill this demand. Existing memory devices, which include static random-access memory (SRAM), dynamic random-access memory (DRAM), and Flash memory, have several drawbacks when considering low power consumption and high-density issues; for example, larger footprints are required by SRAM as the single-bit cell area is equivalent to 150 to $300F^2$, where F is the lithography feature size[1,2], periodic refresh is needed by DRAM[3], and limited cycles can be withstood by Flash memory[4,5]. On the other hand, emerging spin-based memory devices that include spin-transfer torque magnetic random-access memory (STT-MRAM)[6–8], and domain wall motion (DWM)-based racetrack memory[9,10], and Skyrmion-based memory[11,12], have the potential to overcome the above-mentioned constraints of conventional memory.

Spin configurations with a stable spatial variation, such as helimagnets and skyrmions, have recently attracted a great deal of interest in the research community as they are promising candidates for magnetic memory, spin-logic devices, and future spintronics applications[13–15]. One type of spatial variation, where magnetic moments are spatially rotating in a plane that is perpendicular to the propagation plane, is known as a bloch-like chiral helimagnet[16]. In a standard micromagnetic system, this chiral helimagnet can be realized by the competition between exchange energy and Dzyaloshinskii–Moriya interaction (DMI) that arises due to a lack of inversion symmetry in non-centrosymmetric materials[17,18]. Upon the application of an external magnetic field, the helical period of the helimagnet can be tuned because the Zeeman energy, which arises upon the external magnetic field, tends to align spins along the applied field direction[19]. In this letter, we propose a memory device structure named as helimagnet-based random-access memory (HMRAM), consisting of a helimagnetic layer sandwiched by two ferromagnetic layers, with the capability of multi-bit storage and non-volatile memory characteristics. The exchange-coupled free layer on one side of the helimagnet (the other side is strictly pinned) can follow the external fields, thus applying controllable torques onto the helimagnet. Once the external magnetic field is removed, the free layer tends to align to its anisotropy axis and lock the helimagnet into predefined configurations. Thus, a non-volatile behavior can be achieved in the helimagnet in the absence of an external magnetic field. This spring-like helimagnet can be tuned in 180 increments until it can no longer hold more torque. The number of stored bits is therefore determined by the strength of

DMI in the helimagnet and the anisotropy energy in the free layer.

We first show how the helimagnetic layer can be formed as a result of the competition between exchange energy and DMI energy. After that, we examine how a helimagnet period can evolve as a function of DMI energy while maintaining constant exchange stiffness. We then proceed to illustrate the writing mechanism in our proposed memory system. A complete 360-degree cycle rotation of the top free layer as a function of an applied magnetic field is depicted. It is found that the helimagnetic layer follows the free layer and starts twisting in the presence of a magnetic field, while at zero fields, the free layer's anisotropy energy locks the system in non-volatile spin configurations. The non-volatile states' helicity can be increased or decreased by simply rotating the external field in the clockwise or counter-clockwise directions. This way we can write multi-bit memory states and they are stable without an external magnetic field. Since there is a change in the relative spin angle within the helimagnet, reading of the memory states can be done simply by sensing the resistance change as a result of spin scattering[20].

In this research, Object Oriented MicroMagnetic Framework (OOMMF) was used to simulate the dynamics of the magnetization due to its accuracy and acceptance as a standard micromagnetic problem solver[21]. The total magnetic free energy, E, of our system is comprised of various energy densities, including exchange energy density (w_E), DMI energy density (w_D), Anisotropy energy density (w_A), and Zeeman energy density (w_Z). The energy terms selected are in agreement with the experimental evidence of helimagnet[22–24]. Thus, Energy, E, can be written as:

$$E = \int [w_E + w_D + w_A + w_Z] d^3r \tag{1}$$

Exchange energy density, w_E, term can be expressed as:

$$w_E = A[(\nabla m_x)^2 + (\nabla m_y)^2 + (\nabla m_z)^2] \tag{2}$$

where A is the exchange stiffness of the material and m_x, m_y, and m_z are the x,y, and z components of the magnetization vector **m**, respectively. Magnetization vector **m** is defined as the ratio of normal magnetization, M, to the saturation magnetization, M_s. To replicate the layered quantum material that has a strong in-plane exchange while a small out-of-plane exchange component, we have modified the exchange energy extension provided by OOMMF(exchange6ngbr). In the extension, the x,y, and z components are assumed to be equal, whereas in our case, we have considered the x and y component is 100 times higher than the z components in order to simulate the behavior in a 2D layered material. This extension could be provided to the reader upon request.

The next term, DMI energy density, w_D, can be determined by combining all the different possible Lifshitz invariants for the T crystallographic class and defined by the following equation:

$$w_D = D[\mathbf{m}.(\nabla \times \mathbf{m})] \tag{3}$$

where D depends on the structure of the material and the unit is in J/m^2. The theoretical and experimental value of D ranges from -1.5 mJ/m^2 to 10 mJ/m^2[25–27]. In our calculation, we used the OOMMF extension developed by David Cortés-Ortuño et al. in ref.[28,29].

The third term, Anisotropy energy density term, w_A, can be understood as a preference of materials' magnetization towards a certain lattice direction of the crystal, and the preferred axis is known as Easy Axis. This term is expressed as follows:

$$w_A = K[(\mathbf{m}.\mathbf{u})^2] \tag{4}$$

where K is the material-dependent parameter and is usually expressed in J/m^3, and $\mathbf{u}$ is the direction of crystalline anisotropy.

The final term, w_Z, is known as Zeeman energy density, which results from the interaction between the external field and internal magnetic moment. The following equation is used to describe the term:

$$w_Z = \mu_0 M_s[(\mathbf{m}.\mathbf{H})] \tag{5}$$

where H is the amplitude of the external magnetic field direction with a unit of A/m.

Once we define all the system's energy we let our system relax for minimum energy and extract the feature to understand the memory effects. The simulation parameter details of different layers are given in Table. I.

Exchange energy (J) is associated with the interaction between the magnetic moments of neighboring atoms. It is a result of electrons' quantum mechanical exchange interaction, which arises from the Fermi nature of electrons. In a ferromagnet, the exchange energy is responsible for aligning the magnetic moments of neighboring atoms in the same direction, leading to a strong net magnetic moment. This energy can be realized using a continuous model with constant A as given in the Equation. 2. Fig. 1(a) represents the relaxed spin configurations of a typical magnetic system that has only Exchange energy. As expected, after relaxation, all the spins are aligned in the

TABLE I. List of parameters values to realize the HMRAM

Name of the Parameters	Values
Dimension	X: 500nm, Y: 500nm, Z: 120nm
Cell Size	X: 5nm, Y: 5nm, Z: 2nm
DMI, D (J/m^2)	Helimagnet Layer: 2.5×10^{-3}
Anisotropy, K (J/m^3)	Free Layer: 10^6 Pinned Layer: 10^{10}
Exchange Stiffness, A_z (J/m)	Free Layer: 5×10^{-11} Helimagnet Layer: 1×10^{-11} Pinned Layer: 1×10^{-11}
Saturation Magnetization, M_s (A/m)	10^6

FIG. 1. Relaxed spin configurations with (a) Exchange energy term only, (b) DMI energy only, and (c) both Exchange and DMI energy [This figure is constructed by using Mayavi[30]].

same direction. DMI arises from the breaking of inversion symmetry at the atomic scale and can lead to the formation of a non-collinear magnetic structure. In a material with a strong DMI, the magnetic moments of neighboring atoms are arranged in a perpendicular fashion from each other as can be seen in Fig. 1(b).

When both exchange energy and DMI energy are present in a material, they can compete with

FIG. 2. Simulated spin configuration of a magnetic system with a fixed exchange energy and varying DMI energy (units are in mJm^{-2}).

FIG. 3. Writing scheme on our proposed memory with (a) sense path for reading and programming path for writing (following the scheme of Ref.[32]), (b) Anisotropy Axis along with Write Line axis, and (c) Current pulse diagram for writing a complete cycle. [inset shows the proposed memory structure]

each other and stabilizes neighboring spins at a fixed angle. Once the energy of the system is minimized, the competition between these two energy terms leads to the formation of a helimagnet, where the magnetic moments are arranged in a spiral pattern. A portion of a relaxed spin structure is shown in Fig. 1(c). Thus, depending on the relative of DMI with respect to the exchange energy, a helical magnetic structure with different periodicity can be formed.

To get insights into how the helical period of the helimagnet transforms with respect to the DMI energy, a simulation of the helimagnet with different DMI energy and a fixed exchange energy was performed and the result is shown in Fig. 2. The bottom layer is pinned to the x-axis with high anisotropy. As can be seen in the figure, with the increase in DMI energy, the helical period becomes smaller, meaning the helical period is inversely proportional to the DMI energy value. The results obey the equation of zero fields chiral length of a magnetic system and can be written as[31],

$$L(0) \cong \frac{2\pi a J}{D} \tag{6}$$

Where L is the helical period, a is the crystal lattice constant, J is the exchange energy, and D is the DMI energy.

The proposed memory device, Helimagnet-based random-access memory (HMRAM), shown in the inset of Fig. 3(a), consists of a helimagnet layer that is sandwiched between two ferromagnetic layers. The bottom ferromagnetic layer is pinned while the top layer can be rotated with the application of external fields. The thickness of the bottom pinned layer is set to 5 nm, and it is strictly locked in the +x direction with very high anisotropy. As the thickness was very small, to achieve the locking the anisotropy of that layer was set to a large value.

Fig. 3(a) illustrates the proposed writing schemes, which consist of a pass transistor, our proposed single-unit memory cell, electrodes on top and bottom, and two programming word lines that are perpendicular to one another. An electrical connection is formed between the bottom electrode of the memory cell and the ground through a stack of vias that are connected to a pass transistor below.

To write a memory state inside the memory cell, the pass transistor should be in the off state. After that desired current should be sent to the programming word lines (white arrows), and magnetic fields (yellow arrows) perpendicular to the current directions will switch the memory unit to the desired states. As the programming conductors are physically separated from the proposed memory cell, the parasitic delay would be minimized in the proposed writing scheme. Reading the memory state of the proposed cell could be done by turning on the pass transistor and sending a small amount of current through the memory cell and sensing the change in resistance. The easy axis of the ferromagnetic layers and two different programming lines (Word Line1, WL_1, and Word Line2, WL_2) along with their field lines are depicted in Fig. 3(b).

For effective writing of a memory state, the spin configurations of the top layer must be changed by a specific arrangement of the applied current pulses with associated perpendicular magnetic fields. The pulse polarity and amplitude of the two-word lines along with the resultant top-layer spin configurations are illustrated in Fig. 3(c).

Initially, i.e., at time T_0, we assume that the top layer is aligned with the negative x-axis, which is the easy axis of the bit. Next, at T_1, current flows only through the WL_1, producing a perpendicular magnetic field in the y-direction. The produced magnetic field would rotate the top layer configuration due to the Zeeman energy, while the bottom pinned layer spin configuration will not change due to high anisotropy. At the last quarter of the time T_1, WL_2 will be turned on in order to avoid the spin relaxation back to negative x-direction.

At T_2, we need to turn off the current flow through WL_1 and turn on the current for WL_2, resulting in a magnetic field along the x-axis and top layer spin configurations will lock in the same direction due to its anisotropy. The resultant spin configuration is stable even if we turned off both currents.

At T_3, a negative current flows through the WL_1. This results in a magnetic field that aligns the

FIG. 4. Spin configurations of our proposed memory device (a) when sweeping the magnetic field in clockwise (CW) and counterclockwise (CCW) direction and (b) when each corresponding configuration is relaxed without the magnetic field. (c) Schematic illustrations of the resistance states that correspond to the spin configurations without external magnetic field. As the spin configuration of the free layer is locked by the anisotropy energy of the top layer, the corresponding spin configurations will be stable after the CW or CCW rotation of the free layer. Also, spin configuration at T_1, which is a quarter turn rotation from the equilibrium state, T_0, reverts back to its previous state, as shown by Stable State “0”. Similarly, for smaller rotations not exceeding the anisotropy barrier, they would relax back to the previous state as well.

spin configuration of the top layer to the negative y direction. Thus another 90-degree rotation can be achieved. Similar to the previous steps, a negative current is sent through WL_2 before switching off WL_1 current to prevent bit flipping back.

Lastly, at T_4, a negative current will be conducted through WL_2, and a magnetic field in the negative x direction will be generated and flip the top layer towards that direction. Thus, a 360 rotation is achieved. It can be seen from the figure that these 360 rotations of the top layer are in a clockwise (CW) direction. It is worthwhile mentioning that by simply changing the current polarity, we could achieve a 360-degree counter-clockwise (CCW) rotation of the spin.

Now, the writing scheme is modeled in a typical memory cell, where the total thickness was assumed 120nm, with a helimagnet thickness of 95nm, the bottom pinned layer thickness was 5nm, and the Top layer thickness was 20nm. The parameter details were given in Table. I. Whichever direction we apply the magnetic field, a gradual change of the spin configurations was observed and captured in Fig. 4(a). As can be seen from the figure, there is no change in the bottom layer magnetization since the anisotropy energy is dominant over Zeeman energy. The top layer configurations, however, were changed according to the specific writing scheme described in Fig. 3(c). To make things more comparable, the corresponding writing time for the clockwise rotation has been given as a footnote of Fig. 4(a). It is worthwhile to note that illustrated spin configurations are minimized by considering all the energy terms including Zeeman energy. If we start from the equilibrium state, the clockwise rotation increases the helicity period, while the counterclockwise rotation results in a decreased helicity.

Upon finishing the analysis with the magnetic field, the next study was to find out the non-volatile stable memory state without the magnetic field. The spin configurations of the relaxed stable states are shown in Fig. 4(b). As expected, when the top layer spin configurations are perpendicular to the anisotropy axis, upon removing the external fields, it immediately relaxes to the adjacent state with lower anisotropy energy. We define the stable state at T_0 as equilibrium state '0', states in the CW direction with positive state symbols, e.g., +1, +2, and so on, and the states in the CCW direction are denoted with a negative sign, e.g. -1, -2, and so on. In this particular setup, we have found multiple stable states with +6 states in the positive direction and -6 in the negative direction sweep. Thus, we could fit multi-bit of information in each memory units.

Reliable reading of a memory state is also crucial as real application depends on how easily and reliably we can read and write. In order to read the state of the memory cell, the pass transistor must be turned “ON". The helimagnet period changes upon the writing scheme, and so does its resistance. This is due to the increased spin scattering when the relative angles between adjacent spins change[33]. Thus, to read the memory state inside the device structure, a small voltage is applied to the device and measures the current from the device, which provides the discrete resistance state of the device.

In conclusion, a memory device structure, consisting of a helimagnetic element sandwiched by two ferromagnetic layers(a pinned layer and a free layer), with the capability of multi-bit and non-volatile data storage has been proposed. In order to tune the helical period of the memory cell, a rotating in-plane external magnetic field, resulting from two word lines, was used in CW and CCW direction to increase and decrease the helical period from the equilibrium state. The spin configurations were stabilized by the anisotropy of the free layer when the external field was removed and the states are non-volatile. The reading scheme of the memory is done through the different resistance states for different memory states due to spin scattering. Overall, the proposal of our memory device paves the path for future spin-based emerging memory.

ACKNOWLEDGMENTS

This work was supported by the Natural Sciences and Engineering Research Council (NSERC) of Canada Discovery grant No. RGPIN-2022-03753, and the Canada First Research Excellence Fund - Transformative Quantum Technologies(TQT). The authors would like to thank Professor Lin Tan for her support with access to the 'deepgpu0.eng.uwaterloo.ca' server. Marijan Beg would like to acknowledge the UK Skyrmion Project - EPSRC Programme Grant (EP/N032128/1)

AUTHOR DECLARATIONS

CONFLICT OF INTEREST

The authors have no conflicts to disclose.

DATA AVAILABILITY STATEMENT

The data that support the findings of this study are available from the corresponding author upon reasonable request.

AUTHOR CONTRIBUTIONS

Rabiul Islam: Conceptualization (equal); Formal analysis (lead); Investigation (lead); Methodology (lead); Data curation (lead); Validation (lead); Visualization (lead); Writing – original draft (lead); Writing – review & editing (lead).

Peng Li: Conceptualization (supporting); Visualization (supporting); Methodology (supporting); Writing – review & editing (supporting).

Marijan Beg: Methodology (supporting), Visualization (Supporting), Writing – review & editing (supporting), Formal analysis (supporting).

Manoj Sachdev: Supervision (equal); Visualization (supporting); Writing – review & editing (supporting).

Guo-Xing Miao: Conceptualization (lead); Methodology (supporting); Visualization (Supporting); Writing – original draft (supporting); Writing – review & editing (lead); Funding acquisition (lead); Project administration (lead); Resources (lead); Supervision (lead); Validation (equal).

REFERENCES

[1]S. Yu, *Semiconductor Memory Devices and Circuits* (CRC Press, 2022).

[2]B. Rawat and P. Mittal, International Journal of circuit theory and applications **49**, 1435 (2021).

[3]K. K.-W. Chang, D. Lee, Z. Chishti, A. R. Alameldeen, C. Wilkerson, Y. Kim, and O. Mutlu, in *2014 IEEE 20th International Symposium on High Performance Computer Architecture (HPCA)* (IEEE, 2014) pp. 356–367.

[4]S. Boboila and P. Desnoyers, in *FAST* (2010) pp. 115–128.

[5]S. Gerardin, M. Bagatin, A. Paccagnella, K. Grürmann, F. Gliem, T. Oldham, F. Irom, and D. N. Nguyen, IEEE Transactions on Nuclear Science **60**, 1953 (2013).

[6]A. D. Kent and D. C. Worledge, Nature nanotechnology **10**, 187 (2015).

[7]S. Bhatti, R. Sbiaa, A. Hirohata, H. Ohno, S. Fukami, and S. Piramanayagam, Materials Today **20**, 530 (2017).

[8]R. Islam, B. Cui, and G.-X. Miao, Journal of Vacuum Science & Technology B, Nanotechnology and Microelectronics: Materials, Processing, Measurement, and Phenomena **38**, 050801 (2020).

[9]S. S. Parkin, M. Hayashi, and L. Thomas, Science **320**, 190 (2008).

[10]S. Parkin and S.-H. Yang, Nature nanotechnology **10**, 195 (2015).

[11]A. Fert, V. Cros, and J. Sampaio, Nature nanotechnology **8**, 152 (2013).

[12]N. Nagaosa and Y. Tokura, Nature nanotechnology **8**, 899 (2013).

[13]A. Hirohata, K. Yamada, Y. Nakatani, I.-L. Prejbeanu, B. Diény, P. Pirro, and B. Hillebrands, Journal of Magnetism and Magnetic Materials **509**, 166711 (2020).

[14]Y. Cao, Z. Huang, Y. Yin, H. Xie, B. Liu, W. Wang, C. Zhu, D. Mandrus, L. Wang, and W. Huang, Materials Today Advances **7**, 100080 (2020).

[15]M.-G. Han, J. Garlow, Y. Kharkov, L. Camacho, R. Rov, J. Sauceda, G. Vats, K. Kisslinger, T. Kato, O. Sushkov, *et al.*, Science Advances **6**, eaax2138 (2020).

[16]J. ichiro Kishine and A. Ovchinnikov (Academic Press, 2015) pp. 1–130.

[17]I. E. Dzyaloshinskii, Soviet Physics JETP **10**, 628 (1960).

[18]T. Moriya, Physical review **120**, 91 (1960).

[19]J. Chovan and N. Papanicolaou, “Commensurate and incommensurate magnetism in layered antiferromagnets,” in *Frontiers in Magnetic Materials*, edited by A. V. Narlikar (Springer Berlin Heidelberg, 2005) pp. 347–384.

[20]P. Li, R. Islam, G.-X. Miao, and et al., “Helimagnet behavior in Mn1/4TaS2,” (2023), (In a helimagnet Mn-TaS2, we observed multi-resistance states with external fields, corresponding to the helicity change of the system, Manuscript in preparation).

[21]M. Donahue, “Oommf user’s guide, version 1.0,” (1999).

[22]A. Tonomura, X. Yu, K. Yanagisawa, T. Matsuda, Y. Onose, N. Kanazawa, H. S. Park, and

Y. Tokura, Nano letters **12**, 1673 (2012).

[23] C. Zhang, J. Zhang, C. Liu, S. Zhang, Y. Yuan, P. Li, Y. Wen, Z. Jiang, B. Zhou, Y. Lei, *et al.*, Advanced Materials **33**, 2101131 (2021).

[24] M. Beg, R. Carey, W. Wang, D. Cortés-Ortuño, M. Vousden, M.-A. Bisotti, M. Albert, D. Chernyshenko, O. Hovorka, R. L. Stamps, *et al.*, "Ground state search, hysteretic behaviour and reversal mechanism of skyrmionic textures in confined helimagnetic nanostructures," (Nature Publishing Group UK London, 2015) p. 17137.

[25] M. Shen, X. Li, Y. Zhang, X. Yang, and S. Chen, Journal of Physics D: Applied Physics **55**, 213002 (2022).

[26] A. Hrabec, N. Porter, A. Wells, M. Benitez, G. Burnell, S. McVitie, D. McGrouther, T. Moore, and C. Marrows, Physical Review B **90**, 020402 (2014).

[27] M. Beg, M. Albert, M.-A. Bisotti, D. Cortés-Ortuno, W. Wang, R. Carey, M. Vousden, O. Hovorka, C. Ciccarelli, C. S. Spencer, *et al.*, Physical Review B **95**, 014433 (2017).

[28] D. Cortés-Ortuño, M. Beg, V. Nehruji, R. Pepper, and H. Fangohr, "Oommf extension: Dzyaloshinskii-moriya interaction (dmi) for crystallographic classes t and o," (2018).

[29] D. Cortés-Ortuño, M. Beg, V. Nehruji, L. Breth, R. Pepper, T. Kluyver, G. Downing, T. Hesjedal, P. Hatton, T. Lancaster, *et al.*, New Journal of Physics **20**, 113015 (2018).

[30] P. Ramachandran and G. Varoquaux, Computing in Science & Engineering **13**, 40 (2011).

[31] Y. Togawa, T. Koyama, K. Takayanagi, S. Mori, Y. Kousaka, J. Akimitsu, S. Nishihara, K. Inoue, A. Ovchinnikov, and J.-i. Kishine, Physical review letters **108**, 107202 (2012).

[32] B. Engel, J. Akerman, B. Butcher, R. Dave, M. DeHerrera, M. Durlam, G. Grynkewich, J. Janesky, S. Pietambaram, N. Rizzo, *et al.*, IEEE Transactions on Magnetics **41**, 132 (2005).

[33] L. Wang, N. Chepiga, D.-K. Ki, L. Li, F. Li, W. Zhu, Y. Kato, O. S. Ovchinnikova, F. Mila, I. Martin, D. Mandrus, and A. F. Morpurgo, Phys. Rev. Lett. **118**, 257203 (2017).

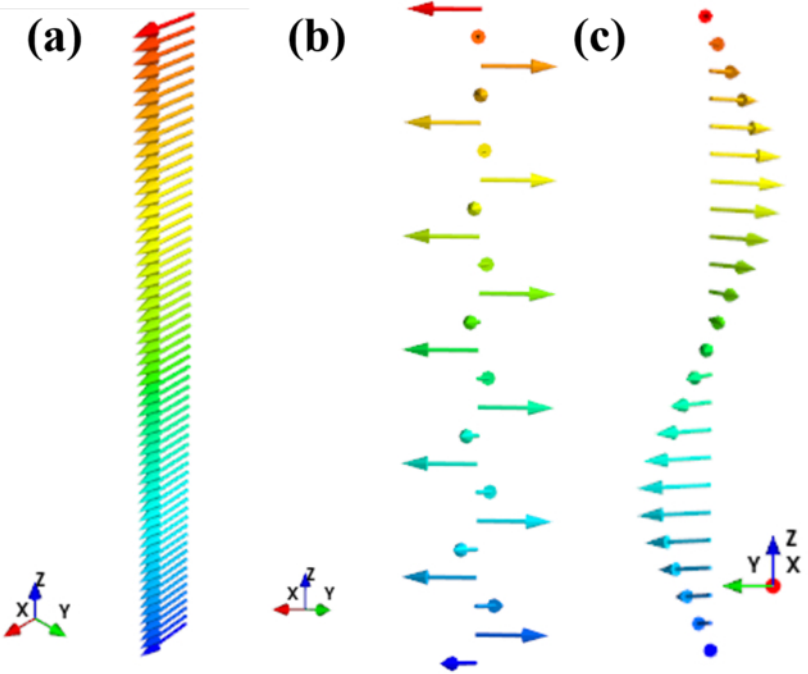
(a)
Z
X
Y
(b)
Z
X
Y
(c)
Z
Y
X

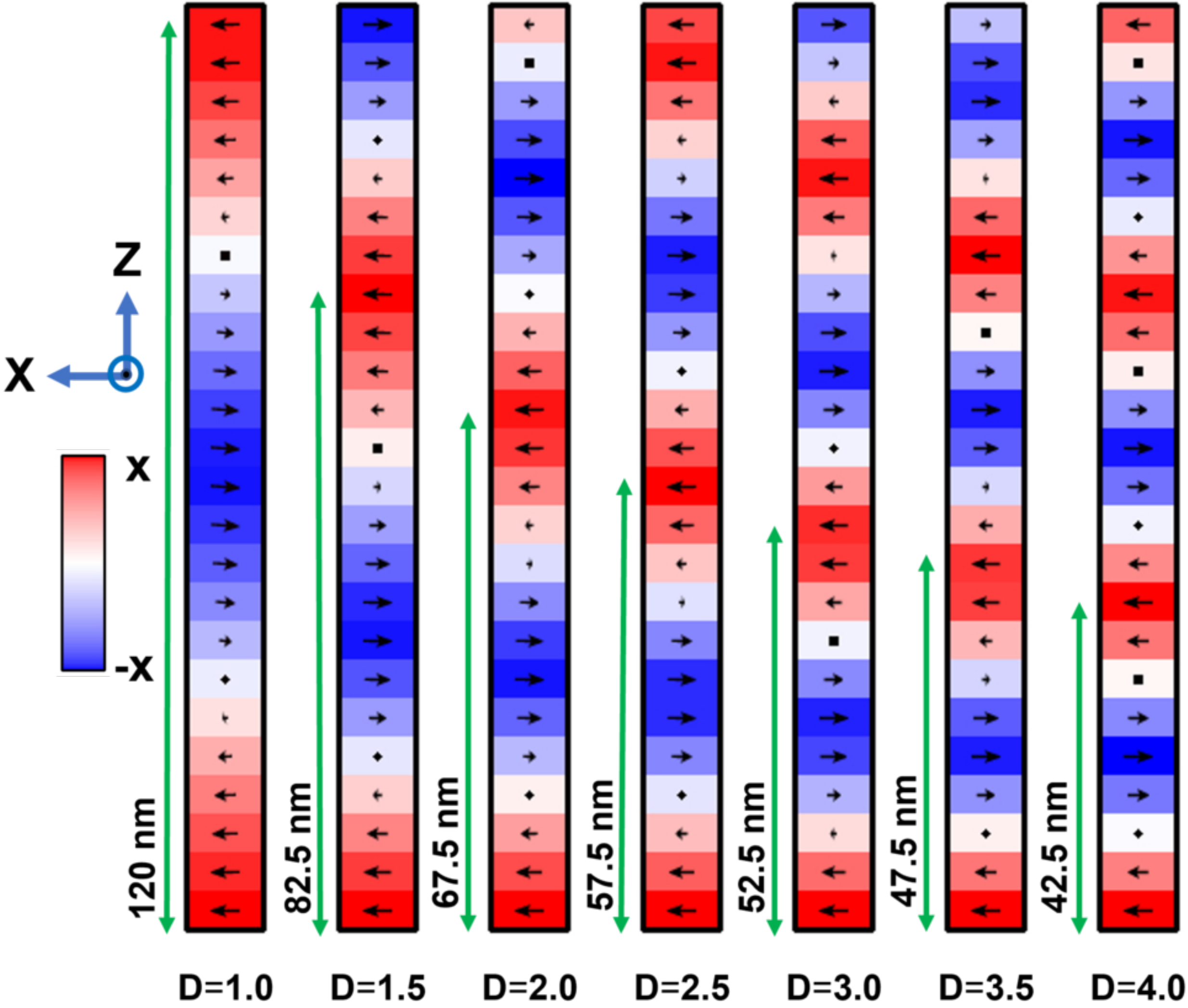
Z
X
x
-x
120 nm
82.5 nm
67.5 nm
57.5 nm
52.5 nm
47.5 nm
42.5 nm
D=1.0
D=1.5
D=2.0
D=2.5
D=3.0
D=3.5
D=4.0

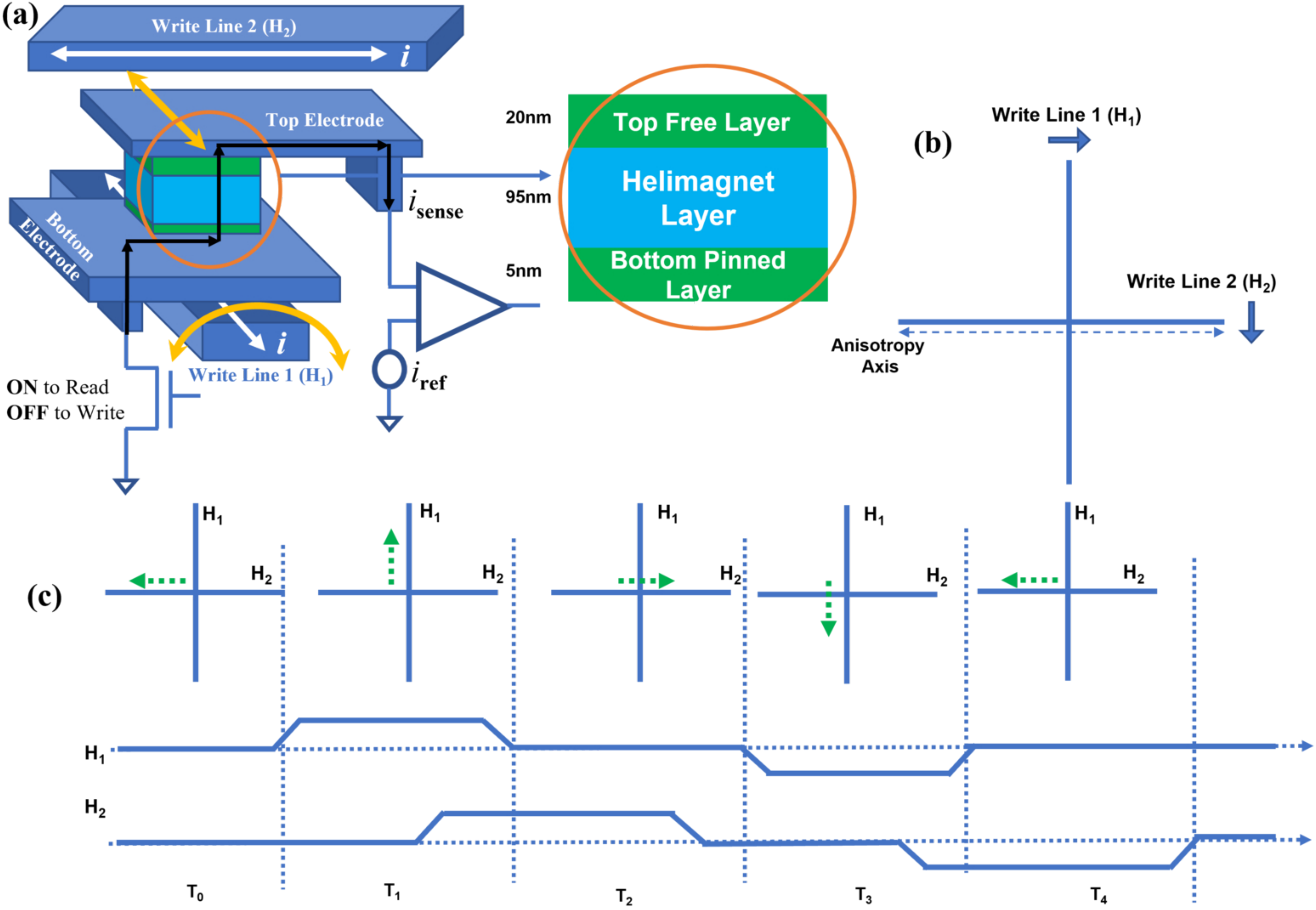
(a)
Write Line 2 (H_2)
i
Top Electrode
Bottom Electrode
i
Write Line 1 (H_1)
ON to Read
OFF to Write
i_{sense}
i_{ref}
20nm
95nm
5nm
Top Free Layer
Helimagnet Layer
Bottom Pinned Layer
(b)
Write Line 1 (H_1)
Write Line 2 (H_2)
Anisotropy Axis
(c)
H_1
H_2
H_1
H_2
H_1
H_2
H_1
H_2
H_1
H_2
H_1
H_2
T_0
T_1
T_2
T_3
T_4

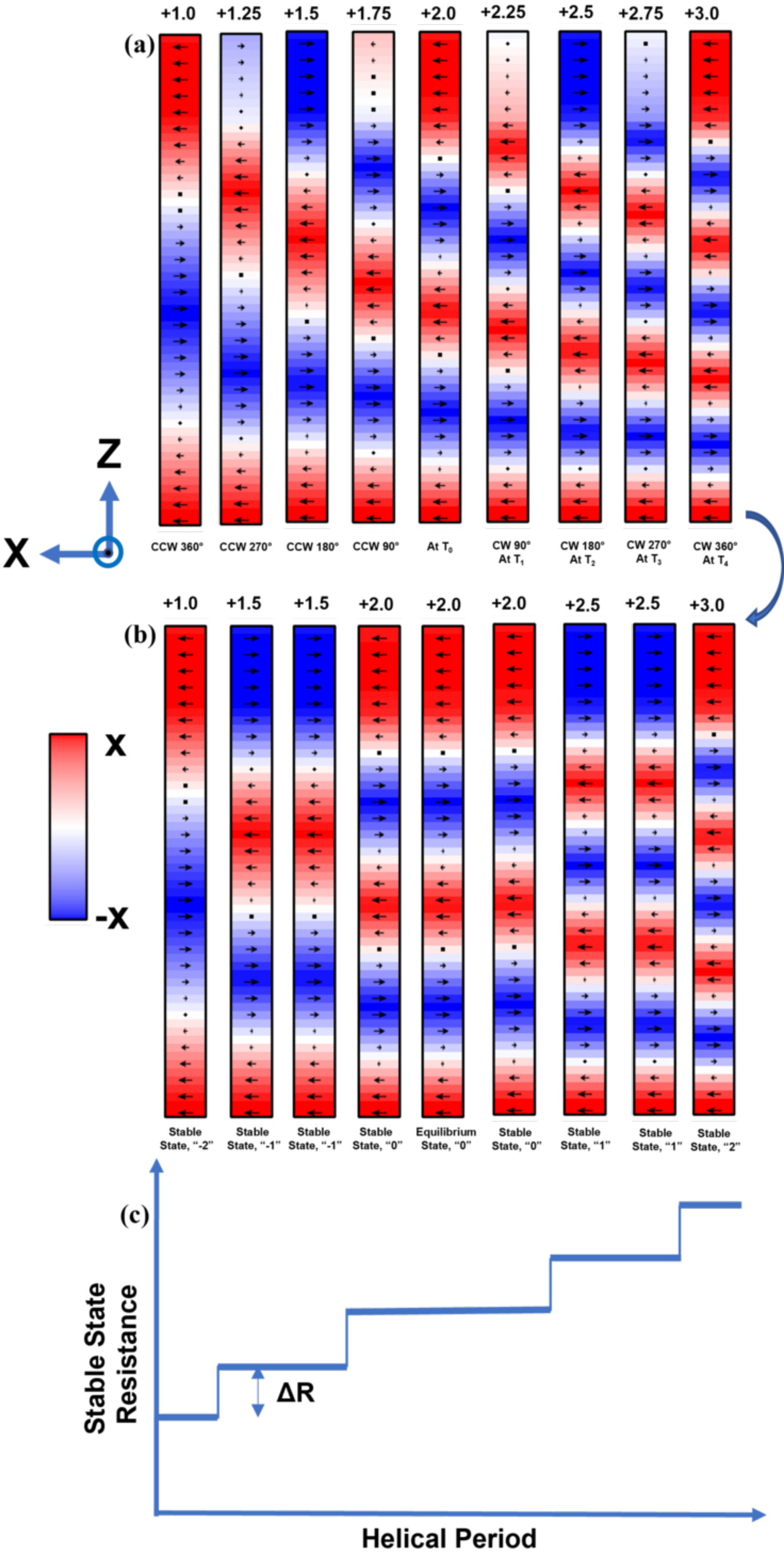
+1.0
+1.25
+1.5
+1.75
+2.0
+2.25
+2.5
+2.75
+3.0
(a)
Z
X
CCW 360°
CCW 270°
CCW 180°
CCW 90°
At T0
CW 90° At T1
CW 180° At T2
CW 270° At T3
CW 360° At T4
+1.0
+1.5
+1.5
+2.0
+2.0
+2.0
+2.5
+2.5
+3.0
(b)
X
-X
Stable State, "-2"
Stable State, "-1"
Stable State, "-1"
Stable State, "0"
Equilibrium State, "0"
Stable State, "0"
Stable State, "1"
Stable State, "1"
Stable State, "2"
(c)
Stable State Resistance
ΔR
Helical Period